World Applied Sciences Journal 33 (1): 01-13, 2015
ISSN 1818-4952

DOI: 10.5829/idosi.wasj.2015.33.01.14569

# Investigation of Torsional Behaviour of High-Strength Reinforced Concrete Sections

[1]*Ahmed Hassan* and [2]*Laila Abd-EL Hafez*

[1]Civil Engineering Department, Faculty of Engineering, Beni-Suef University, Egypt
[2]Civil Engineering Department, Faculty of Engineering, El-Minia University, Egypt

**Abstract:** This paper presents a parametric study on the behaviour of high-strength reinforced concrete (HSC) sections subjected to pure torsion using nonlinear finite element analysis. This study used the results from a previous experimental program to verify the investigated models. The investigated models were designed according to the Egyptian Code of Practice recommendations. The investigated factors were a reduction in the steel reinforcement from 100% to 50%, the presence of compression forces in torsion, a reduction in the concrete cross section from a factor of 1 to a factor of 0.69, variable concrete compressive strength between 45 and 90 N/mm$^2$ and variable box section wall thickness. Test results showed that the pre-cracking and post–cracking stiffness decreases and the angle of twist at cracking and failure torque increases with a reduction in steel. A reduction in the concrete section size also has major effects on the general behaviour of sections subjected to torsion, increasing the cracking and decreasing the failure torque.

**Key words:** Torsion · Nonlinear analysis · High strength concrete

## INTRODUCTION

The application of high-strength concrete with compressive strength in excess of 41 MPa [1] has gained wide acceptance in the construction industry and is currently being used in many parts of the world. Generally, reinforced concrete members may be subjected to bending, shear and torsion, sometimes in combination. Torsion is a very important factor to be considered in the analysis of high strength reinforced concrete HSRC sections. Three-dimensional torsional behaviour becomes complicated once concrete cracking occurs and elastic theory is no longer applicable [2, 3]. Current design methods continue to be based, in many respects, on the empirical approach, using the results of a large amount of experimental data. However, the finite element method lends itself to these circumstances [4-5]. The analyses of reinforced concrete, its behaviour and the behaviour of box sections were approached using finite element analysis [6-8]. The reliability of the finite element models used in these studies must be carefully examined beforehand [9]. Statically indeterminate torsion, in which the torsion cannot be determined from statics and the twist alone, is required for deformational compatibility between interconnecting elements [10-12]. Cracking of a HSC beam was more brittle than that of a NSC beam [13, 14].

The number of cracks at failure in HSC and NSC beams is approximately the same and the maximum crack width at failure increases as the concrete strength increases [14]. The total twist angle at failure of NSC and HSC beams are the same and the modulus of elasticity and torsional stiffness of HSC are higher than that of NSC [15]. The peak strain of HSC is influenced by the type, shape, size of aggregate and suggested an equation for predicting strain [16]. The determination of the torsional capacity of reinforced concrete beams uses the theory described [17, 18], based on the stress block factors (β, α) for compressive strength up to 110 MPa (modified stress block factors (SBF)). The torsional capacity of under-reinforced beams is independent of concrete strength [18]. Longitudinal reinforcement was more effective than transverse reinforcement in controlling crack width. The minimum amount of reinforcement defined by the American concrete institute ACI Committee [20] is inadequate for equilibrium torsion of

**Corresponding Author:** Ahmed Hassan, Civil Engineering Department, Faculty of Engineering, Beni-Suef University, Egypt.

high-strength reinforced concrete beams. The different Codes used for the design of reinforced concrete sections subjected to torsional moments were developed to calculate suitable dimensions and reinforcement of sections. The first formula was mentioned in the Egyptian Code for design and construction of concrete structures [19], in which the design of a section subjected to torsion is based on the space truss theory. Equation (1) is developed by the Egyptian Code for design and construction [19].

$$qtu = \frac{Tu}{2Ao * te} \quad \text{Eq. 1}$$

$$Astr = \frac{Tu * \varepsilon}{2 * A0 * (\frac{Fyst}{\gamma s})} \quad \text{Eq. 2}$$

$$Asl = \frac{Astr * ph}{\varepsilon} * \frac{Fyst}{fy} \quad \text{Eq. 3}$$

The second formula was developed by ACI [20] based on the space truss theory equation and are presented in equation (4):

$$\sqrt{\left(\frac{V_u}{b_w d}\right)^2 + \left(\frac{T_u p_h}{1.7 A_{oh}^2}\right)^2} \leq \varphi\left(\frac{V_c}{b_w d} + 0.66\sqrt{f_c^{'}}\right) \quad \text{Eq. 4}$$

$$Tu = \frac{0.9*2*Ao*Ast*Fyst}{s} \cot\theta \quad \text{Eq. 5}$$

$$Asl = \frac{Astr}{s}\frac{fyst}{fy} \cot 2\theta \quad \text{Eq. 6}$$

The third formula was introduced in British standards [21] based on the space truss theory equation and is presented in equation (7)

$$qu = \frac{2*Tu}{b^2 * (t\frac{b}{s})} \quad \text{Eq. 7}$$

$$Asv = \frac{Tu*s}{0.95*x1*y1*0.80*fyst} \quad \text{Eq. 8}$$

$$Asl = \frac{Asv}{s} * \frac{fyst}{fy} (x1+y1) \quad \text{Eq. 9}$$

According to this research, verified by the experimental program presented by Mohamed [22], the effects of five parameters are investigated. A reduction in steel reinforcement from 100% to 50% is studied, along with a change in the concrete cross section size at factors of 1, 0.87, 0.81 and 0.69 of the cross section area, while maintaining the aspect ratio. The increase in compressive strength from 45 $N/mm^2$ to 90 $N/mm^2$ is investigated, the presence of compression forces in torsional behaviour is studied and the effect of the box section's wall thickness is studied.

**Research Significance:** In high-strength reinforced concrete structures, many members are subjected to a torsional moment by means of the load condition or element shape. Many codes depend on the space truss theory, which gives limited data about the torsional behaviour of HSRC sections, given torsion assumptions. Many variables were studied to obtain more information as pre-cracking torsional stiffness, cracking torque, post-cracking torsional stiffness, angle of twist at cracking, steel response and failure torque, to obtain optimum understanding of the torsional behaviour of concrete sections.

**Methodology:** The methodology adopted in this research is based on finite element modelling. These models will be developed using the ANSYS finite element software package. The verification of the finite element models is based on previously reported experimental results [22]. A theoretical program was designed to study the effect of torsional moment on concrete section behaviour. Varying concrete cross sections, compressive strength, compression force and box section dimensions were investigated to assess their effect on concrete sections subjected to a torsional moment. A Solid 65 element is used to model the concrete element. This element is defined by eight nodes with three degrees of freedom at each node, with translations in the nodal x, y and z directions, as shown in Fig 1. The link 8 element is used to model the steel reinforcement. Two nodes are required for this element. Each node has three degrees of freedom, with translations in the nodal x, y and z directions. The link8 element is a uniaxial tension-compression element, as shown in Fig 2. The convergence tolerance was set to 0.001 of the displacement, with a maximum of 15 iterations to reduce the accumulation forces from iteration.

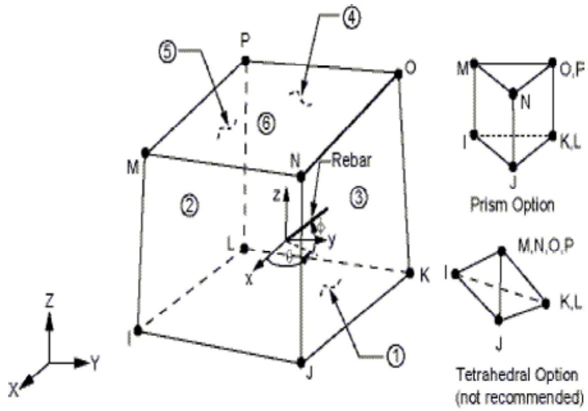


Fig. 1: Solid65 3-D concrete element

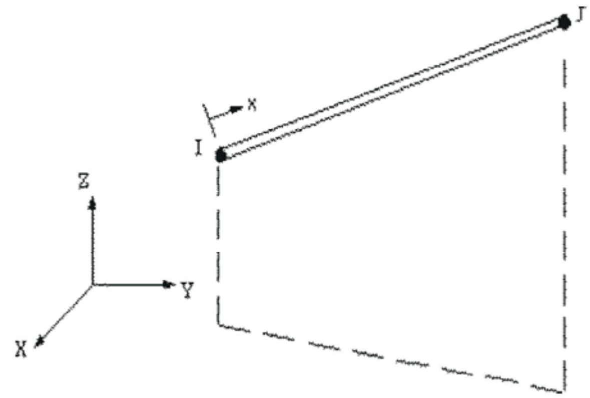


Fig. 2: Link8 3-D par element.

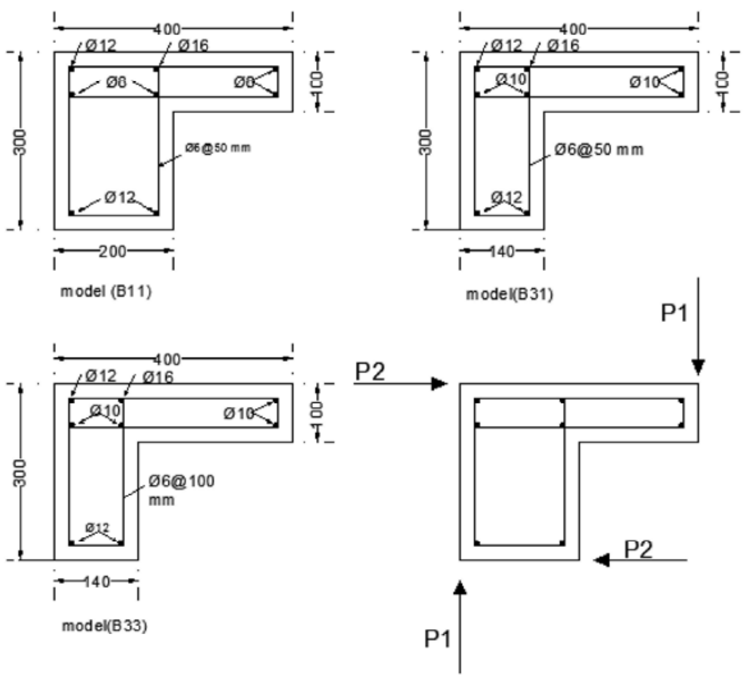


Fig 3: Details of the steel reinforcement and loading system for analysed beams.

The Newton-Raphson approach is the iterative process adopted by ANSYS to solve nonlinear equations. In this approach, the load is subdivided into a series of load increments. The load increments can be applied over several load steps. Before each solution, the Newton-Raphson approach evaluates the out-of-balance load vector, which is the difference between the restoring forces (the loads corresponding to the element stresses) and the applied loads. The program then calculates a linear solution using the out-of-balance loads and checks for convergence. If the convergence criteria are not satisfied, the out-of-balance load vector is re-evaluated, the stiffness matrix is updated and a new solution is obtained. This iterative procedure continues until the problem converges. The full Newton-Raphson solution procedure, which is used in the present analysis, is the default method for performing this type of analysis.

**Verification:** The experimental program from previous work reported by Mohamed [22] consisted of a series of tests on reinforced concrete beams fixed at the base, with L-sections subjected to pure torsion. Results of beams (B11, B31 and B33) were used to verify the model used in solving torsion problems. Details of the reinforcement, loading system and boundary conditions for selected beams are shown in Figs 3 and 4. The material properties of the analysed beams as reported by Mohamed [22] are given in Table 1. Poisson's ratio was assumed to be 0.18

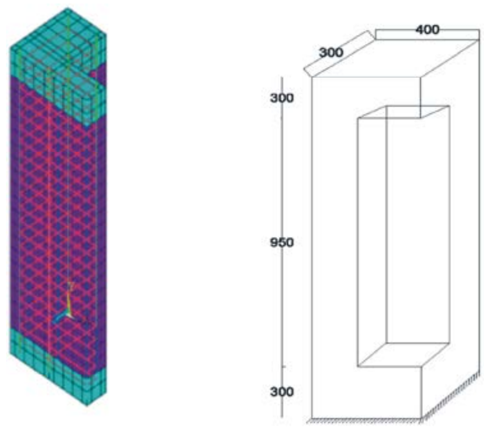


Fig. 4: Boundary conditions for beams and the mesh of the analysed beam.

Table 1: Material properties for the beams reported by Mohamed [22].

| Beam NO | Fcu $N/mm^2$ | Ft $N/mm^2$ | Ec $KN/mm^2$ | S Mm | Fy $N/mm^2$ 6 mm | 8 mm | 10 mm | 12 mm | 16 mm | Es $KN/mm^2$ 6 mm | 8mm | 10 mm | 12 mm | 16 mm |
|---|---|---|---|---|---|---|---|---|---|---|---|---|---|---|
| $B_{11}$ | 42.8 | 2.9 | 23.0 | 50 | 465 | 536 | 500 | 518 | 542 | 180 | 214 | 206.6 | 199.2 | 181 |
| $B_{13}$ | 40.7 | 2.8 | 20.7 | 100 | | | | | | | | | | |
| $B_{14}$ | 52.3 | 3.2 | 23.0 | 50 | | | | | | | | | | |

Table 2: Comparison between theoretical analysis and reported experimental results

| Model no. | $Tcr_{theor}/Tcr_{Exp}$ | $Tf_{theor}/Tf_{Exp}$ | $\theta cr_{theor}/\theta cr_{Exp}$ | $\theta f_{theor}/\theta f_{Exp}$ | $\epsilon f_{theor}/\epsilon f_{Exp}$ |
|---|---|---|---|---|---|
| $B_{11}$ | 0.97 | 0.98 | 1.20 | 0.87 | 1.05 |
| $B_{13}$ | 1.01 | 1.08 | 1.01 | 1.11 | 1.10 |
| $B_{14}$ | 1.03 | 1.03 | 0.98 | 0.75 | 1.26 |

for concrete and 0.3 for steel. All analysed beams are fixed at the base. It can be concluded that the ANSYS program model is capable of providing a good prediction of the overall behaviour of the beam under pure torque [8]. The shear retention factor is an important parameter in the analysis of torsional problems; a value of 0.25 is recommended for use in this analysis [3]. The cracking torque is sensitive to the value used for tensile strength of concrete.

Table 2 summarizes the comparisons between the experimental and theoretical results for B11, B13 and B14. Figs 5-10 show a comparison between the experimental and theoretical results for the torque vs. angle of twist, torque vs. stirrup steel strain and torque vs. longitudinal steel strain curves. The predicted results compare reasonably well with the experiments. Different values for the shear retention factor of open cracks are used (0.1, 0.25, 0.3 and 0.4). In Fig 5, comparisons are presented for Torque vs. Angle of twist for values of the shear retention factor of opened cracks. These comparisons show that predicted results compare well with the experiments for a shear retention factor of 0.25 for opened cracks. This value was also recommended in previous work reported by Mostofinejad and Talaeitaba

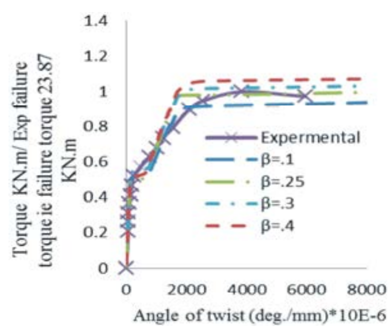


Fig. 5: Torque vs Angle of twist of B11, by the open shear transfer coefficient

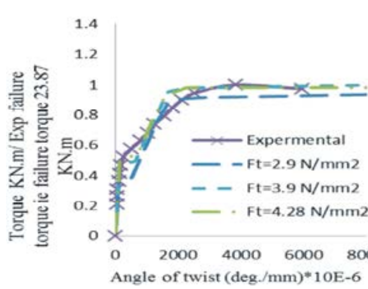


Fig. 6: Torque vs Angle of twist of B11, by uniaxial tensile strength, with open shear transfer coefficient β=.25"

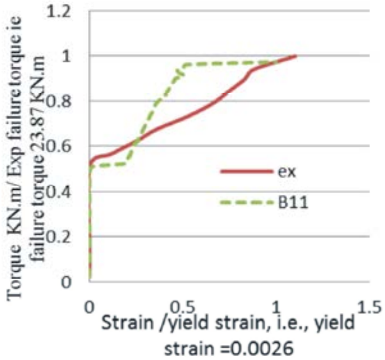


Fig. 7: Strain in longitudinal steel, comparison between experimental and theoretical results for B11.

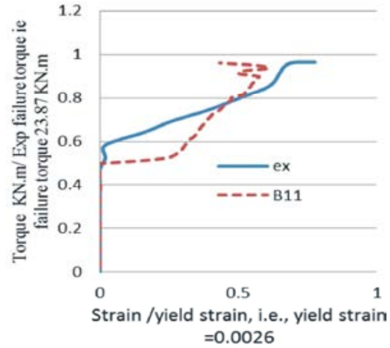


Fig. 8: Strain in stirrups, comparison between experimental and theoretical results for B11

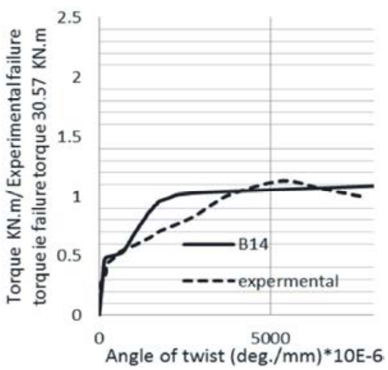


Fig. 9: Torque vs. Angle of twist curve, comparison between experimental and theoretical results for B14

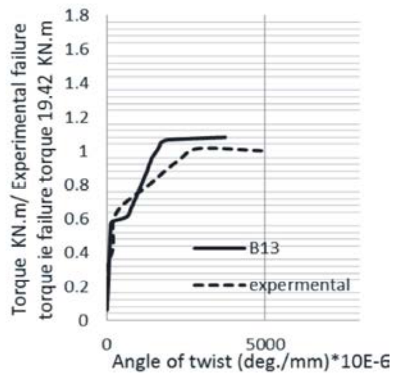


Fig. 10: Torque vs. Angle of twist curve, Comparison between experimental and theoretical results for B13

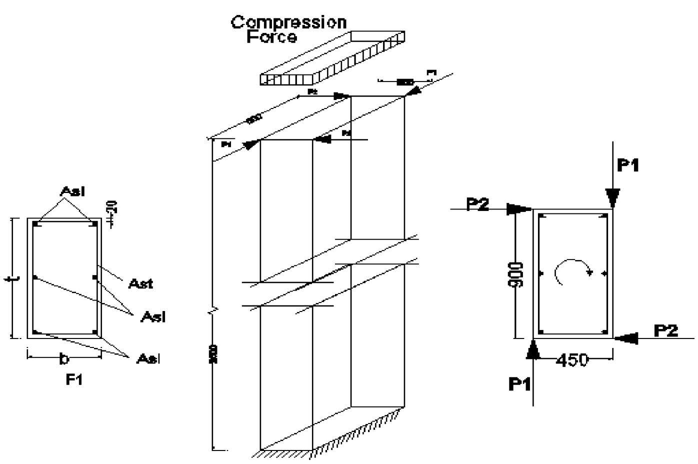


Fig. 11: Details of group F, where the main variable is the size of the concrete cross section

[3]. The maximum differences in all variables were approximately 12% under-estimation and 5% overestimation. It is well-known that tensile strength has a major effect on the cracking torque. The value reported by Mohamed [22] underestimates the cracking torque of the analysed beam ($B_{11}$). A value of 10% of the reported compressive strength was used as the tensile strength recommended by the ECP (203) in the analysis [19]. Fig. 6 shows the strong correlation between the experimental and analytical curves for a tensile strength of 10% of compression strength.

Table 3: Mechanical properties of the materials used in the analysis

| Beam NO | Fcu N/mm$^2$ | Ft N/mm$^2$ | Ec N/mm$^2$ | Fy long N/mm$^2$ | Fy st N/mm$^2$ | Es N/mm$^2$ |
|---|---|---|---|---|---|---|
| All beams of all groups except group G | 60 | 6 | 34082 | 360 | 240 | 210000 |
| G1 | 45 | 4.5 | 29516 | | | |
| G2 | 75 | 7.5 | 38105 | | | |
| G3 | 90 | 9 | 41742 | | | |

Table 4: Details of the analysed beams

| | | Cross section | | | Reinforcement of stirrups | | Reinforcement of longitudinal steel | | |
|---|---|---|---|---|---|---|---|---|---|
| Group | Beam No | b mm | t mm | Spacing (s mm) | Ast mm$^2$ | εst% | Asl mm$^2$ | εsl% | NOT |
| E | Effect of Reduction of steel (stirrups & longitudinal) for the same cross section | | | | | | | | |
| | E1 | | | | 83.63 | 0.28 | 914.35 | 0.51 | Reduction of Ast=.9$Ast_{(control)}$ |
| | E2 | | | | 74.33 | 0.25 | 812.756 | 0.45 | Reduction of Ast=.8$Ast_{(control)}$ |
| | E3 | 300 | 600 | 100 | 65.04 | 0.22 | 711.161 | 0.40 | Reduction of Ast=.7$Ast_{(control)}$ |
| | E4 | | | | 55.75 | 0.19 | 609.567 | 0.34 | Reduction of Ast=.6$Ast_{(control)}$ |
| | E5 | | | | 46.46 | 0.15 | 507.972 | 0.28 | Reduction of Ast=.5$Ast_{(control)}$ |
| F | Effect of size of concrete cross section. | | | | | | | | |
| | F1 | 280 | 560 | 100 | 108.41 | 0.39 | 1098.54 | 0.70 | Ac section= 0.87$Ac_{(control)}$ |
| | F2 | 270 | 540 | | 117.65 | 0.44 | 1145.1 | 0.79 | Ac section = 0.81$Ac_{(control)}$ |
| | F3 | 250 | 500 | | 140.1 | 0.56 | 1251.2 | 1.00 | Ac section = 0.69$Ac_{(control)}$ |
| G | Effect of compressive strength. | | | | | | | | |
| | G1 | 300 | 600 | 100 | 92.92 | 0.3 | 1015.94 | 0.56 | Fcu=45 N/mm$^2$ |
| | G2 | | | | | | | | Fcu=70 N/mm$^2$ |
| | G3 | | | | | | | | Fcu=90 N/mm$^2$ |
| H | Effect of torque combined with compression force | | | | | | | | |
| | H1 | 300 | 600 | 100 | 92.92 | 0.3 | 1015.94 | 0.56 | Force/Area= 1.0 N/mm$^2$ |
| | H2 | | | | | | | | Force/Area= 1.5 N/mm$^2$ |
| | H3 | | | | | | | | Force/Area= 2.0 N/mm$^2$ |
| | H4 | | | | | | | | Force/Area= 4.0 N/mm$^2$ |
| I | The effect of box section wall thickness. | | | | | | | | |
| | I1 | 300 | 600 | 100 | 92.92 | 0.3 | 1015.94 | 0.56 | The wall thickness=120 mm |
| | I2 | | | | | | | | The wall thickness=100 mm |
| | I3 | | | | | | | | The wall thickness=80 mm |
| | I4 | | | | | | | | The wall thickness=60 mm |

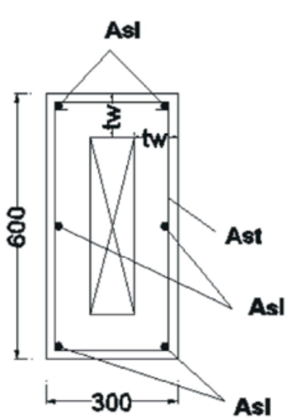


Fig. 12: Details of a steel reinforced beam for group I, where the main variable was the box section wall thickness

**Theoretical Analyses of the Models (Parametric Study):** After verification and obtaining a strong agreement between experimental and theoretical results, the theoretical study was performed using the well-known ANSYS structural software, which is based on the nonlinear finite element method. The study cases were chosen to on the overall behaviour of high-strength concrete beams under torsion and designed according the ECP (203) [19] study cases consisting of 19 beams. The studied beams' details, loading and boundary conditions are shown in Fig 11. The mechanical properties of the materials used in the analysis of different groups are given in Table 3. All analysed beams had same Poisson's ratio of 0.18 for concrete and 0.3 for steel. The shear transfer coefficients of 0.25 for opened cracks and 0.8 for closed cracks were used in all analysed beams.

The geometric and steel reinforcement details of these beams are given in Table 4 and divided into five groups. The first group investigated the effect of steel reduction (stirrups and longitudinal steel) for the same cross section. By adjusting four identical beams in the cross section and the spacing between stirrups, the steel was reduced from 100% to 50% of the $A_{st}$ of the control beam. The second group investigated the size effect of concrete cross sections using a control beam cross section reduced to 69% of the original, with the same aspect ratio. The third group investigated the compressive strength of concrete, with values of 45 N/mm$^{2,}$ 75 N/mm$^2$ and 90 N/mm$^2$. The fourth group shows the effect of wall thickness in box sections, as shown in Fig. 12. The box section wall thicknesses were 120 mm, 100 mm, 80 mm and 60 mm. The fifth group investigated the effect of torque, combined with a normal force of 1, 1.5, 2 and 4 N/mm$^2$. All analysed beams were fixed at the base.

## RESULTS

**Overall Behaviour as Reflected in Torque vs Angle of Twist Curves:** One of the most important effects of the torsion moment on the concrete section is the angle of twist. The ECP does not give a limitation for the rotation angle, so this ratio is helpful. Torque to design torsional moment is reported against angle of twist to assess the concrete section torsional behaviour for all study cases. The first group addresses a reduction of up to 50% of the steel area. The angle of twist at cracking torque was approximately 5.0% of the angle of twist at failure torque. The behaviour is essentially linear up to the cracking torque. At constant torque of 1.3 times design torque, the angle of twist increased to approximately 40% of the angle of twist at failure torque. Steel reinforcement did not significantly contribute to this stage. At failure, a 50% reduction in the steel area increased the twist angle by approximately 25%, as shown in Fig 13. Reducing the concrete cross section area has a major effect on torsional behaviour and a significant effect on the cracking torque. The slopes of the initial linear part of the torque vs. twist angle curve increased with an increase in the twist angle and a reduction in torsional capacity. Reducing the cross section area to 0.69 of the control section affected pre-cracking torsional stiffness by approximately 60%. Reducing the cross section size has a minor effect on the value of the angle of twist at cracking and failure. All analysed models had the same behaviour and trend for a percentage reduction in design torque, as shown in Fig 14. With compressive strength varying from 45 to 90N/mm$^2$, the torque vs. twist angle curve has approximately the same linear trend in the first stage. The twist angle in the pre-cracking stage increased by 100% when compressive strength was increased to 90 N/mm$^2$. There is a slight effect on the angle of twist at cracking and a significant effect at failure, as shown in Fig. 15. Normal force enhanced the torsional capacity of the concrete sections and reduced the angle of twist, as

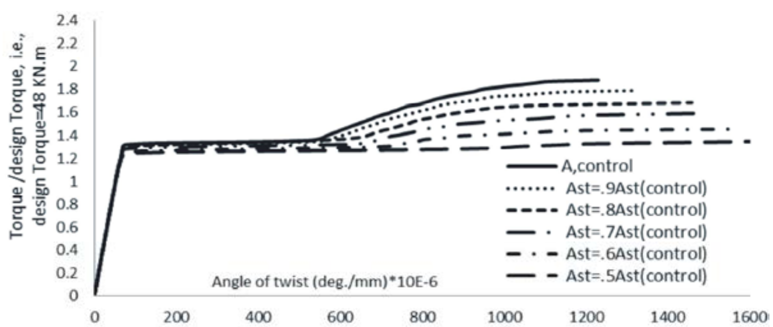


Fig. 13: Torque vs. Angle of twist of group E, where the main variable was a reduction in steel

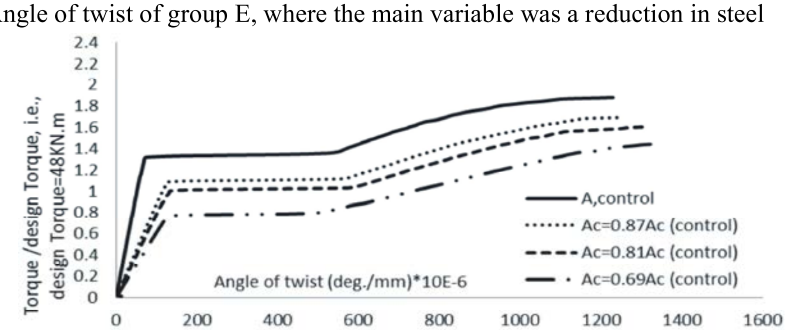


Fig. 14: Torque vs. Angle of twist of group F, where the main variable was a reduction in the size of the concrete section

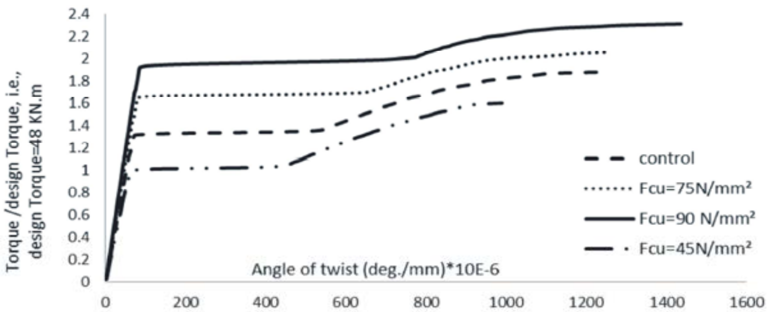


Fig. 15: Torque vs. Angle of twist of group G, where the main variable was compressive strength

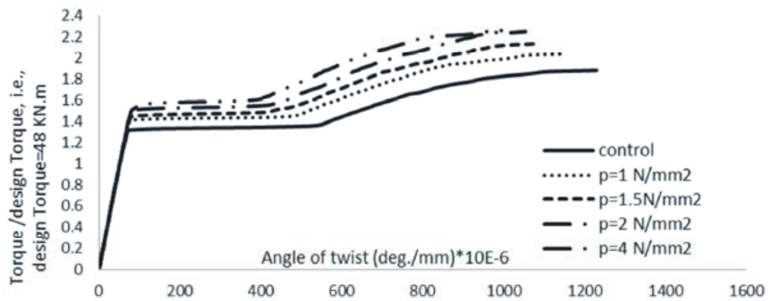


Fig. 16: Torque vs. Angle of twist of group H, where the main variable was the compression force on the section.

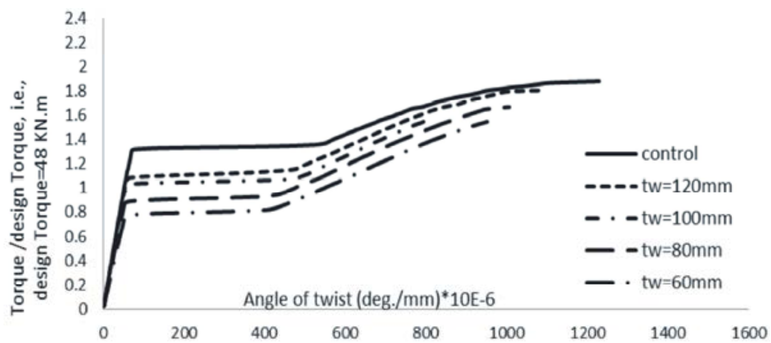


Fig. 17: Torque vs. Angle of twist of group I, where the main variable was the wall thickness of the box section.

shown in Fig 16. The slope of the initial linear part of the torque vs. twist angle curve is not affected by compression stress. Compression stress has a major effect on the cracking torque. Compression stress also has a major effect on post-cracking torsional stiffness, as the applied compression force increases the post-cracking torsional stiffness by approximately 30%. A box section is a section with good torsional stiffness, designed to resist torsion moment. The wall thickness of a box section directly affects the cracking, failure torque and angle of twist at cracking and failure, as reported in Fig. 17. The slope of the initial linear part of the torque vs. twist angle curve (pre-cracking torsional stiffness) up to the cracking torque is affected by the wall thickness of the box section. The wall thickness of the box section has a major effect on the slope of the second part of the curve (post-cracking torsional stiffness).

**Effect of Torsional Moment on Steel Response:** The steel reinforcement in a concrete section plays an important role on section torsional behaviour, especially after cracking of the concrete. Mid-span longitudinal steel strain on the long side of the concrete cross section was recorded along with torque to understand the behaviour of steel reinforcement in a concrete section subjected to torsion. For all models, no strains were observed on the longitudinal steel before cracking. After cracking, large increases in steel strains were observed to approximately 0.4 of steel yield strains. The reduction of steel reinforcement (stirrup and longitudinal) has a major effect on torque carrying capacity. A 50% reduction in steel reduced the torsional capacity of the section to approximately 25%, as shown in Fig. 18. The section torsional capacity does not show a significant improvement after a steel reduction of 50% and shows

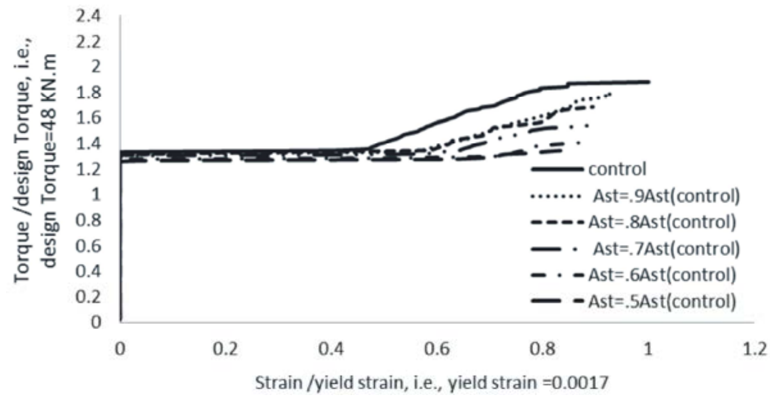


Fig. 18: Torque vs. longitudinal steel strain by reduction of steel, group (E).

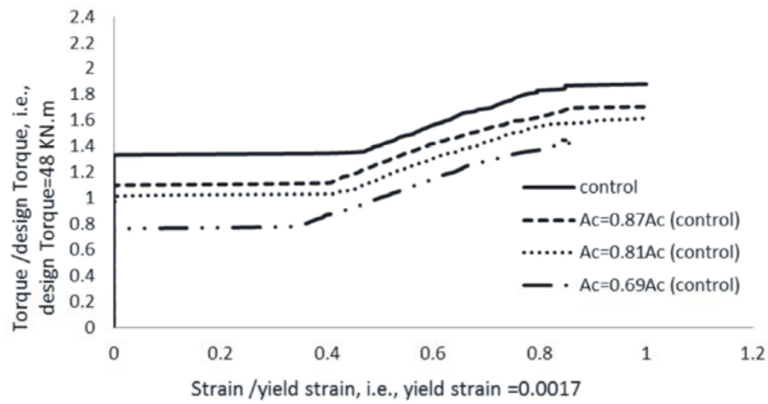


Fig. 19: Torque vs. longitudinal steel strain by reduction of concrete section size.

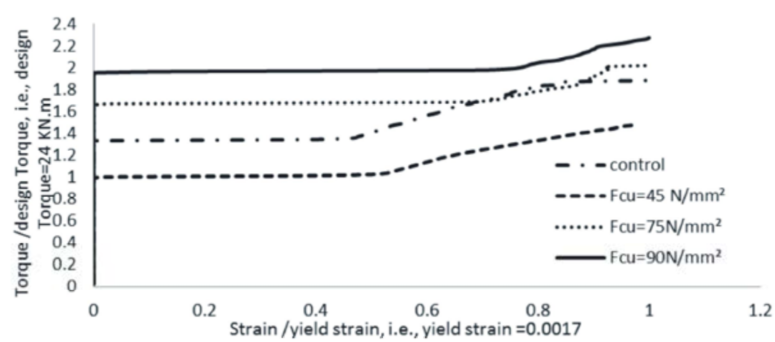


Fig. 20: Torque vs. longitudinal steel strain by concrete compressive strength.

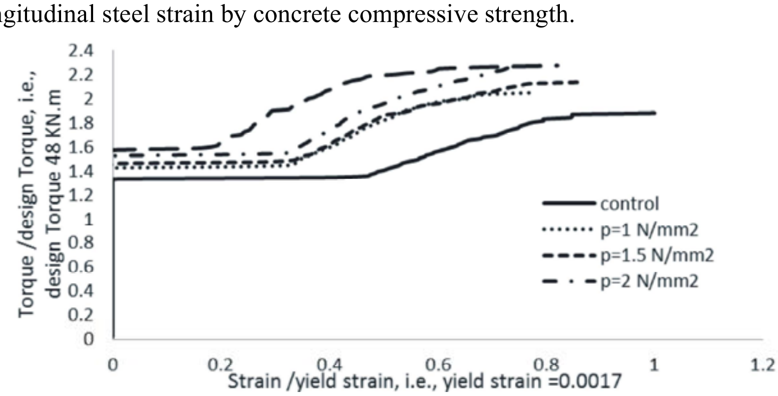


Fig. 21: Torque vs. longitudinal steel strain by compression force.

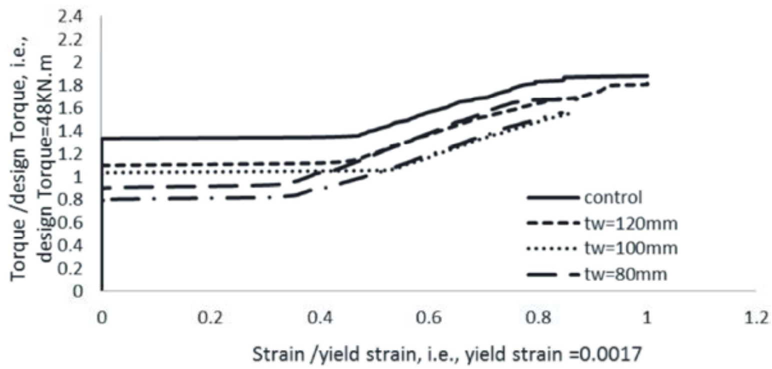


Fig. 22: Torque vs. longitudinal steel strain by box section wall thickness, group (I).

increased steel strain. After the size of the concrete cross section was reduced, large increases in steel strains were observed after cracking. At failure, the steel strain reached 100% of its yield strains. The reduction of cross section has a major effect on torsional capacity of the longitudinal steel after cracking, as reported in Fig. 19. Varying the compressive strength delayed the steel strains and increased the torsional section capacity before cracking by 100%, as shown in Fig. 20. After cracking, large increases in steel strains were observed, up to 50% of yield strain. At failure, steel carried approximately 100% of its yield strain. Compressive strength has a major effect on the torque carrying capacity of the longitudinal steel after cracking. Increased compression force and torsional moment after cracking caused large observed decreases in steel strains. At failure, the steel carried approximately 85% of its yield strain, depending on the applied compressive force, as shown in Fig. 21. Compression stress had a major effect on the torque carrying capacity of the longitudinal steel after cracking, as the applied compressive force enhanced the concrete strength. Increasing the box section wall thickness increased the torsional capacity of concrete sections to 55% at cracking and 30%at failure, as shown in Fig. 22. After cracking, large increases in steel strains were observed.

## DISCUSSION

In all results of the parametric study, the pre-cracking torsional stiffness behaviour is essentially linear before cracking. The reinforced concrete members of the rectangular cross sections behave like plain concrete members before cracking, regardless of the amount of torsional reinforcement. The pre-cracking torsional stiffness was almost the same for analysed beams of group E, G and H, with different reinforcement contents when the cross section was the same, as shown in Table 5, but there is a clear effect of the size of the concrete section (group F) on the value of pre-cracking torsional stiffness. As the concrete section size decreases, the pre-cracking torsional stiffness decreases and this leads to the fact that the size of the concrete section has a major effect on torsional behaviour. In the case of cracking torque, the reinforcement does not significantly contribute to the behaviour before cracking. However, the cracking torque does increase slightly with the increase in the amount of steel, shown by group (E). In the case of pure torque, the tensile principle stress, which causes the first crack, is equal parts shear stress due to applied torque (when compressive stress exists, the tensile principle stress is a function of shear stress due to torque) and compressive stress due to applied compressive force. The existence of compression stress on the section affects the cracking torque and increasing the compression stress increases the cracking torque, as seen in group (H). Reducing the size of the concrete section of group (F) decreased the cracking torque. Increasing the wall thickness increased cracking torque in group (I). Post-cracking torsional stiffness was also studied; torsional stiffness is greatly reduced after cracking occurs. Table 5 shows the comparison between post-cracking stiffness for all modules relative to the control. The post-cracking stiffness portion of the torque-twist curve isn't fully linear, due to the continuous process of crack propagation, followed later by the yielding of steel and crushing of concrete. The average value of the post-cracking stiffness is approximately 20% from the pre-cracking stiffness. Reducing steel reinforcement and concrete sections has a clear effect on the post-cracking torsional stiffness for groups (E) and (F), but the compressive strength of concrete has a minor effect on the post-cracking torsional stiffness, as seen in group (G). Increased compression force improves the section properties after cracking. As the compression

Table 5: Theoretical results of the parametric study for all beams

| Group | Beam No | Kpr/Kpr control | Tcr/Tcr control | Kpo/Kpo control | Angle of twist | | Steel strain/ Steel strain control | | Tf/Tf control |
|---|---|---|---|---|---|---|---|---|---|
| | | | | | ?cr/?cr control | ?f/?f control | At 0.87Tf | At Tf | |
| E | E1 | 1.00 | 0.98 | 0.94 | 0.97 | 1.07 | 0.92 | 0.96 | 0.95 |
| | E2 | 1.00 | 0.97 | 0.75 | 0.96 | 1.19 | 0.89 | 0.96 | 0.89 |
| | E3 | 1.00 | 0.96 | 0.66 | 0.93 | 1.20 | 0.88 | 0.89 | 0.85 |
| | E4 | 1.00 | 0.94 | 0.34 | 0.91 | 1.27 | 0.87 | 0.86 | 0.78 |
| | E5 | 1.00 | 0.92 | 0.24 | 0.90 | 1.37 | 0.85 | 0.86 | 0.72 |
| F | F1 | 0.45 | 0.81 | 0.88 | 1.81 | 1.01 | 1.00 | 0.94 | 0.90 |
| | F2 | 0.40 | 0.74 | 0.86 | 1.86 | 1.07 | 1.00 | 0.94 | 0.85 |
| | F3 | 0.32 | 0.58 | 0.63 | 1.93 | 1.09 | 0.85 | 0.94 | 0.77 |
| G | G1 | 0.87 | 0.76 | 1.05 | 0.94 | 0.80 | 1.00 | 0.71 | 0.85 |
| | G2 | 1.12 | 1.24 | 0.60 | 1.16 | 1.02 | 1.00 | 1.07 | 1.09 |
| | G3 | 1.22 | 1.43 | 0.43 | 1.23 | 1.17 | 1.00 | 1.17 | 1.23 |
| H | H1 | 1.00 | 1.06 | 1.03 | 1.07 | 0.93 | 0.77 | 0.64 | 1.08 |
| | H2 | 1.00 | 1.08 | 1.09 | 1.09 | 0.88 | 0.76 | 0.71 | 1.13 |
| | H3 | 1.00 | 1.14 | 1.11 | 1.16 | 0.86 | 0.74 | 0.73 | 1.20 |
| | H4 | 1.00 | 1.16 | 1.19 | 1.23 | 0.84 | 0.74 | 0.86 | 1.46 |
| I | I1 | 0.96 | 0.81 | 1.02 | 0.88 | 0.89 | 1.00 | 1.10 | 0.96 |
| | I2 | 0.93 | 0.77 | 1.02 | 0.78 | 0.88 | 0.85 | 1.17 | 0.93 |
| | I3 | 0.86 | 0.65 | 1.02 | 0.75 | 0.82 | 0.85 | 0.89 | 0.89 |
| | I4 | 0.75 | 0.57 | 1.02 | 0.71 | 0.77 | 0.82 | 0.93 | 0.82 |

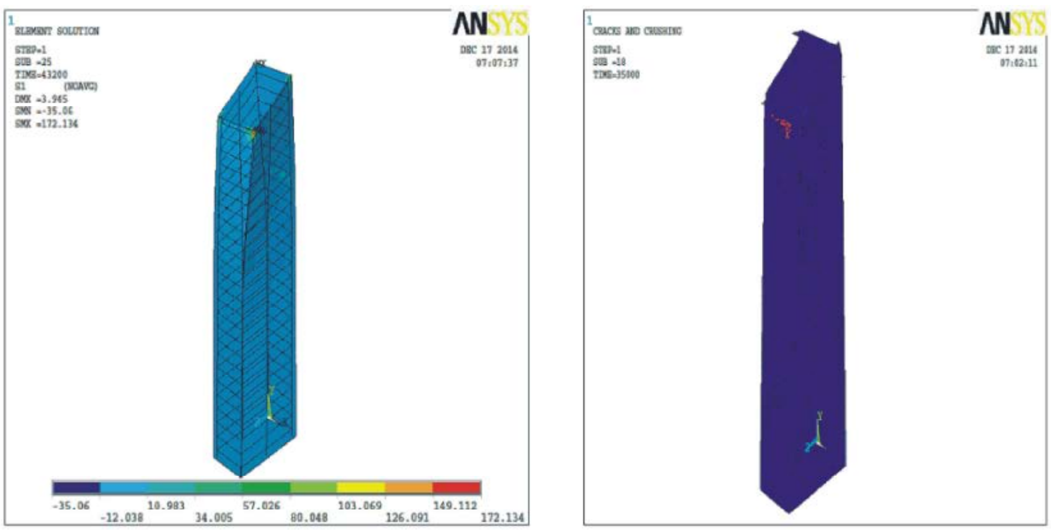


Fig. 23: Deformed shape after applying load.

force on the cross section increases, the post-cracking torsional stiffness increases. The wall thickness has a great effect on the post-cracking stiffness; increasing wall thickness increased post-cracking stiffness in group (I). Fig. 23 illustrates the deformed shape of the beams after applying loads.

## CONCLUSIONS

- Reducing the steel reinforcement of a section subjected to torsion and designed according to ECP 203 has a significant effect on the cracking and ultimate failure torque, increasing the cracking and decreasing the failure torque. The pre-cracking and post–cracking stiffness also decrease and the angle of twist at cracking and failure increases. Reducing the steel reinforcement by up to 20% has a minor effect on the torsional behaviour of beams.
- Reducing the size of the concrete section has a major effect on the general behaviour of sections subjected to torsion, increasing cracking and decreasing failure torque. The angle of twist at cracking and failure increases, to a greater degree than with a reduction in steel reinforcement.

- Increasing the compressive strength of concrete improves ductility, cracking torque and ultimate torque for the same cross section. Increasing the compressive strength by 30% increases the failure torque by 40%.
- Applying compression force on the cross section improves the cracking torque, ductility and ultimate torque for the same cross section, with the ultimate torque increasing by 15% for 1 $N/mm^2$ pressure.
- The ECP 203 design equations for sections subjected to torsion overestimate the required area of steel, as it is based on the lower bound of the space truss theory.
- For box sections, the wall thickness affected the first stage of loading more than it affected the failure stage.

Notations

| | |
|---|---|
| Astr | area of one leg of stirrups |
| $A_{sl}$ | area of longitudinal steel |
| $A_{sv}$ | area of two legs of closed links at a section |
| b | smaller dimension of a rectangular section |
| $b_w$ | width of section |
| $f_c$ | compressive strength of concrete |
| $F_{yst}$ | yield stress of stirrups |
| $F_y$ | yield stress of the longitudinal steel |
| $K_{po}$ | post-cracking torsional stiffness |
| $K_{pr}$ | pre-cracking torsional stiffness |
| P | load subjected to the element |
| $P_c$ | outer perimeter of concrete cross section |
| $p_h$ | perimeter of the outer stirrups |
| qtu | shear stress due to torsion |
| qu | shear strength of concrete |
| s | spacing between stirrups |
| t | thickness of the section |
| Tcr | cracking torque |
| $Tcr_{Exp}$ | cracking torque - experimental |
| $Tcr_{theor}$ | cracking torque - theoretical |
| $t_e$ | thickness of the thin-walled tube |
| $T_f$ | failure torque |
| $T_{f\ Exp}$ | failure torque - experimental |
| $T_{ftheor}$ | failure torque - theoretical |
| $T_u$ | ultimate torsional stresses |
| Vu | shear force at section |
| x1 | shorter centre-to-centre dimensions of the closed stirrups |
| y1 | longer centre-to-centre dimensions of the closed stirrups |
| $\beta$ | shear transfer coefficient in open cracks |
| $\gamma s$ | steel strength reduction factor |
| $\varepsilon sl$ | percentage of area of longitudinal steel in the section |
| $\varepsilon st$ | percentage of area of stirrups in the section |
| e | steel strain |
| $ef_{Exp}$ | steel strain at failure torque - experimental |
| $ef_{Theor}$ | steel strain at failure torque - theoretical |
| el | longitudinal steel strains |
| ells | long leg stirrups strain |
| esls | short leg stirrups strain |
| $qcr_{Exp}$ | angle of twist at the cracking torque - experimental |
| $qcr_{theor}$ | angle of twist at the cracking torque - theoretical |
| $qf_{Exp}$ | angle of twist at the failure torque - experimental |
| $qf_{theor}$ | angle of twist at the failure torque - theoretical |

## REFERENCES


1. ACI Committee 363, 1992. State-of-the-Art Report on High-Strength Concrete. (ACI 363R-92), American Concrete Institute, Detroit, pp: 59.
2. Hsu Thomas, T.C., 1984. Torsion of Reinforced Concrete. Van Nostrand Reinhold, New York.
3. Mostofinejad, D.A. and S.B.B. Talaeitaba, 2011. Nonlinear Modeling of RC Beams Subjected to Torsion using the Smeared Crack Model. The Twelfth East Asia-Pacific Conference on Structural Engineering and Construction, 14: 1447-1454.
4. Segerlind Larry, J., 1984. Applied Finite Element Analysis. John Wiley and Sons, New York.
5. Anthony, J. and B.S. Wolanski, 2004. Flexural Behavior Of Reinforced And Prestressed Concrete Beams Using Finite Element Analysis, MSc. Thesis submitted to the Faculty of the Graduate School, Marquette University, Milwaukee, May.
6. Daniel, J. Ridley-Ellis John S. Owen and Gwynne Davies, 2002. Theoretical and measured torsional behaviour of Rectangular Hollow Sections. International Offshore and Polar Engineering Conference Kitakyushu, Japan, ISSN 1098-6189 May.
7. Tan, E.L. and B. Uy, 2009. Experimental Study on Straight Composite Beams Subjected to Combined Flexure and Torsion. Journal of Constructional Steel Research, 65: 784-793.
8. Hsu Thomas, T.C., 1990. Shear Flow Zone in Torsion of Reinforced Concrete. Journal of Structural Engineering, 116(11): 25246.
9. Taher W. Abd-El Rahman and Laila M. Abd-EL Hafez, 2014. Reliability of Egyptian code of practice equations to design reinforced concrete sections under static short time torque. El-Minia Unversity, Egypt, July.
10. Ghoneim Mashhour Ahmed, 2008. Design of reinforcement concrete structures. Cairo University, Egypt, Vol 1, Chapter 8.
11. Kaminski, M. and W. Pawlak, 2011. Load Capacity And Stiffness of Angular Cross Section Reinforced Concrete Beams Under Torsion. Wroclaw University of Technology, XI(4): 885-903.
12. Pawlakn, W. and M. Kamin´ski, 2012. Cracking Of Reinforced Concrete Beams Under Torsion-Theory and Experimental Research. Elsevier Urban & Partner, 12: 368-375.

13. Rasmussen, L.J. and G. Baker, 1995. Torsion in Reinforced Normal and High Strength Concrete Beams -Part 1: Experimental test series. ACI Structural Journal, 92: 56-62.
14. Victor, D.J. and R. Muthukrishnan, 1973. Effect of stirrups on ultimate torque of reinforced concrete beams. ACI Journal Proceeding, 70(4): 300-306.
15. Rasmussen, L.J., G. Baker, 1995.Torsion in reinforced normal and high strength concrete beams. Part-I: an experimental test series. ACI Structural J., 92(1):56-62.
16. Rasmussen, L.J. and G. Baker, 1994. Assessment of torsional strength in reinforced normal and high-strength concrete beams. Aust. Civil Eng. Trans., IE Aust., 36(2): 165-71.
17. Koutchoukali, N.E. and G. Belarbi, 2001. Torsion of high strength reinforced concrete beams and minimum reinforcement requirement. ACI Structural J., 98(4): 462-9.
18. Abdalkader A. Mohammed, 2012. Predicating of Torsional Strength of Reinforced Concrete Beams Using Artificial Neural Network. The Iraqi Journal for Mechanical and Material Engineering, 12(4): 694-708.
19. ECP 203-07, 2007. Egyptian code of practice for Design and Construction of Concrete Structures. Cairo, Egypt, Chapter 4.
20. ACI Committee 318M-05, Building Code Requirements For Structural Concrete Andcommentary. American Concrete Institute Farmington Hills, Michigan.
21. BS 8110-2:1985, 2001. British Standard Structural Use of Concrete", Part 2: Code of Practice for Special Circumstances, BSI Publications,.
22. Mudathir Sulieman Mohamed, 1986. A finite Element And Experimental study Of Rinforced Concrete in Torsion. Ph.D. Thesis, Dept. of Civil Engineering, University of Glasgow.